Amino acid transport in thermophiles: Characterization of an arginine-binding protein from Thermotoga maritima. 3. Conformational dynamics and stability

ARTICLE *in* JOURNAL OF PHOTOCHEMISTRY AND PHOTOBIOLOGY. B, BIOLOGY · NOVEMBER 2012

Impact Factor: 2.96 · DOI: 10.1016/j.jphotobiol.2012.11.004 · Source: PubMed

7 AUTHORS, INCLUDING:

Alessio Ausili
Universidad Técnica Particular de Loja
41 PUBLICATIONS **297** CITATIONS
SEE PROFILE

Dimitrios Fessas
University of Milan
73 PUBLICATIONS **1,397** CITATIONS
SEE PROFILE

Journal of Photochemistry and Photobiology B: Biology 118 (2013) 66–73

Contents lists available at SciVerse ScienceDirect

Journal of Photochemistry and Photobiology B: Biology

journal homepage: www.elsevier.com/locate/jphotobiol

Amino acid transport in thermophiles: Characterization of an arginine-binding protein from *Thermotoga maritima*. 3. Conformational dynamics and stability

A. Ausili [a,*], A. Pennacchio [a], M. Staiano [a], J.D. Dattelbaum [b], D. Fessas [c], A. Schiraldi [c], S. D'Auria [a,*]

[a] Laboratory for Molecular Sensing, IBP-CNR, Naples 80131, Italy
[b] Department of Chemistry, University of Richmond, Richmond, VA 23173, USA
[c] Università di Milano, DeFENS, Milan, Italy

ARTICLE INFO

Article history:
Received 17 October 2012
Received in revised form 7 November 2012
Accepted 8 November 2012
Available online 29 November 2012

Keywords:
Fluorescence
Phosphorescence
Arginine
Extremophiles
Unfolding
Thermodynamics

ABSTRACT

Arginine-binding protein from *Thermotoga maritima* (TmArgBP) is a 27.7 kDa protein possessing the typical two domain structure of the periplasmic binding protein family. The protein is characterized by high specificity and affinity for binding a single molecule of L-arginine.

In this work, the effect of temperature and/or guanidine hydrochloride on structure and stability of the protein in the absence and in the presence of L-arginine has been investigated by differential scanning calorimetry, far-UV circular dichroism and intrinsic tryptophan phosphorescence and fluorescence. The results revealed that TmArgBP undergoes an irreversible one-step thermal unfolding process in a cooperative mode. The TmArgBP melting temperature was recorded at 115 °C. The presence of L-arginine did not change the protein secondary structure content as well as the intrinsic phosphorescence and fluorescence protein properties, even if it increases the structural stability of the protein.

The obtained results are discussed in combination with a detailed inspection of the three-dimensional structure of the protein.

1. Introduction

Periplasmic binding proteins (PBPs) constitute a widely distributed protein superfamily involved in the passage of ligands through bacterial cell membranes [1]. In this function, PBPs are associated with ATP-binding cassette (ABC) transport systems, which are multi-protein complexes constituted of two transmembrane domains and two ATP-binding domains that cooperate for nutrient uptake [2,3]. Although PBPs are able to bind many different ligands with diverse degrees of affinity, they show a highly conserved structure. PBPs are single chain polypeptides that appear to be composed of two well defined domains linked by a rotating hinge that can make the protein change its conformation from open to close form and vice versa depending on the absence or presence of ligand [4,5]. Due to the variety of binding specificities, PBPs from *Escherichia coli* have been utilized as design platforms for fluorescent and electrochemical protein biosensors capable of targeting many naturally-occurring ligands, including sugars, anions, and amino acids [6–8]. Arginine-binding protein (ArgBP) is a monomeric protein member of the PBP superfamily and is involved in arginine recruitment and transport; it binds L-arginine with a very high affinity [9]. Here, we have investigated an arginine-binding protein from *Thermotoga maritima* (TmArgBP) a hyper-thermophilic eubacterium originally isolated from various geothermal heated marine sediments with an optimum growth temperature of 80 °C [10]. TmArgBP is an ultra-stable protein with an estimated transition temperature of 116 °C, a monomeric molecular mass of 27.7 kDa and it presents the two domain structure typical of PBPs, each domain consisting of a β-sheet core surrounded by helices [11]. Unlike other arginine-binding proteins, TmArgBP seems to exist not only as monomer but also as dimer and trimer [12], but like all PBPs, the arginine-dependent conformational change (K_d = 20 μM) stabilizes the protein [11,12]. For its characteristics of sensitivity, selectivity and high stability, TmArgBP could be a good potential candidate for the development of an arginine-binding protein-based fluorescent biosensor for real-time and continuous detection of the level of blood arginine that is an important marker of hyper-argininemia, an autosomal recessive disorder of the urea cycle where a deficiency of the enzyme arginase causes a build-up of arginine and ammonia in the blood [13]. Reagentless fluorescent biosensors have the advantage of avoiding the production of secondary components and the modification of the sensor itself [14], for this reason several proteins with these characteristics, in particular from PBP superfamily, have been engineered to make them suitable biosensors, modifying their specificity [15] or conjugating with fluorescent probes [16,17]. In this work, we have investigated the thermodynamic

* Corresponding authors. Address: Institute of Protein Biochemistry, CNR, Via Pietro Castellino, 111, 80131 Napoli, Italy. Tel.: +39 0816132312; fax: +39 0816132273 (A. Ausili), tel.: +39 0816132250; fax: +39 0816132273 (S. D'Auria).
E-mail addresses: a.ausili@ibp.cnr.it (A. Ausili), s.dauria@ibp.cnr.it (S. D'Auria).

1011-1344/$ - see front matter © 2012 Elsevier B.V. All rights reserved.
http://dx.doi.org/10.1016/j.jphotobiol.2012.11.004

and structural characteristics of TmArgBP in the presence and in the absence of L-arginine by means of differential scanning calorimetry, circular dichroism and phosphorescence and fluorescence spectroscopy.

2. Materials and methods

2.1. Materials

Arginine-binding protein from *T. maritima* was cloned, expressed and purified according to previously reported procedures [12]. L-arginine was purchased from Sigma. All other reagents and solvents were commercial samples of the highest purity.

2.2. DSC experiments

Calorimetric measurements were carried out in 5 mM phosphate buffer, pH 7.5, 0.8 mg/ml protein solutions, with a nano DSC (CSC, TA Instruments distributor, USA) apparatus at 0.5 °C/min scan rate in the 10–130 °C range. This instrument uses capillary cells with 0.3 ml sensitive volume. The systems considered were: wild type protein (TmArgBP) alone and TmArgBP in the presence of L-arginine in excess conditions (L-arginine/protein ratio (*r*); *r* = 477). For each system three measurements where performed. A second heating run was also performed (after cooling with the same scan rate) for each system. No signal was observed in the second heating run in both cases indicated that the protein does not refold after thermal denaturation (at least in the time span of the measurements).

Data were analyzed by means of the software THESEUS [18]. The excess molar (monomer) heat capacity $\langle \Delta C_p \rangle$ or $C_P^E(T)$, i.e., the difference between the apparent molar heat capacity $Cp(T)$ of the sample and the molar heat capacity of the "native state", $Cp_{,N}(T)$, was recorded across the scanned temperature range. The methods to treat the raw data (baselines scaling, etc.) are reported elsewhere [19,20]. Suffice here to say that in all cases the signal was rather disturbed in the 25–50 °C range and the apparent denaturation enthalpy $\Delta_d H$ was affected by a rather large error (20–30%) in spite of a very good reproducibility both of the temperature of the denaturation peaks maximum, T_{max}, (that is above 100 °C) and the signal profile. The average values of the apparent denaturation enthalpy $\Delta_d H$ were 680 and 645 kJ mol^{-1} (monomer) for the TmArgBP and TmArgBP with L-arginine systems, respectively.

A possible explanation is that, in our conditions, partial precipitation occurred during the heating run and the effective concentration of the protein in the sensitive volume of the capillary cell became randomly different from the nominal one. Also, the heat capacity drop, $\Delta_d Cp$, across the signal was affected by a rather large error and was therefore not taken into account in the present work. Fortunately the uncertainty in the apparent denaturation enthalpy $\Delta_d H$ did not prevent the thermodynamic analysis (see below) and did not require further experimental efforts to avoid this phenomenon. The theoretical models used to fit the experimental data were tested through the non-linear Levenberg–Marquardt method [21].

2.3. Thermodynamic model

Even in the presence of an irreversible process that prevents the refolding after denaturation, the thermal denaturation of proteins can sometimes be described with a suitable thermodynamic model [27].

Details on the fitting equations of the thermodynamic model used to obtain the parameters presented in Table 1 are reported elsewhere [19]. This model can be formally summarized as a process of dissociation of an oligo- homo-meric protein with concomitant denaturation of the monomers:

$$N_n \overset{K}{\leftrightarrow} nU \tag{1}$$

and the normalized experimental profile can be simulated by the equation:

$$\frac{d\theta}{dT} = \frac{\Delta H^{vH}}{RT^2} \frac{\theta(1-\theta)}{n-\theta(1-\theta)} \tag{2}$$

where θ is the degree of advancement of the total process and can be calculated from the experimental signal (T_i being a pre-denaturation temperature):

$$\theta(T) = \frac{\int_{T_i}^{T} C_p^E(T)}{\Delta_d H} \tag{3}$$

The relevant van't Hoff enthalpy, ΔH^{vH}, can be calculated independently from the experimental data by using the equation:

$$\Delta H^{vH} = (\sqrt{n}+1)^2 RT_{max}^2 C_p^E(T_{max})/\Delta_d H \tag{4}$$

where $C_p^E(T_{max})$ is the excess heat capacity at T_{max}. The van't Hoff enthalpy value calculated with Eq. (4) is expressed per mole of protein considered as an *n*-monomer oligomer. This means that the calculated value has to be divided by *n* to obtain the enthalpy per mole of monomer.

The uncertainty of the calculated ΔH^{vH} was less than 10% in all cases. It is obvious that such a value does not depend on protein concentration errors (see Eq. (4)) since these are included in the common multiplication factor of $C_p^E(T_{max})$ and $\Delta_d H$, so that the relevant ratio is not affected.

Consequently the best fit of the model can be performed either for the normalized signal profile or directly for the experimental data using

$$C_p^E(T) = \Delta_d H \frac{d\theta}{dT} \tag{5}$$

In all cases, the only compatible value of *n* used to obtain a satisfactory fit was *n* = 2.

Table 1
Thermodynamic parameters of the denaturation of TmArgBP at pH 7.0, with and without the presence of L-arginine. Each value is the average of three measurements. The error of temperature T_{max} does not exceed 0.3 °C. The uncertainty of ΔH^{vH} enthalpy is less than 10%.

System	T_{max} (°C)	ΔH^{vH} (kJ mol^{-1})
Wild type	114.9	720
Wild type + L-arginine	118.8	910

We observe that the protein is stabilized in the presence of L-arginine with a slight entropic contribution (increasing the T_{max}) and a substantial enthalpic contribution (increasing the ΔH^{vH}) which suggests a specific binding that may promote conformational changes in the overall protein structure.

2.4. CD measurements

Far-UV (from 260 nm to 190 nm) CD spectra were obtained on a Jasco 810 spectrophotometer under constant nitrogen stream at 20 and 95 °C. An external bath circulator (Julabo F25) was used to maintain the desired temperature controlled by a thermocouple placed directly on the cell holder. Spectra were collected in a 0.1 cm path length quartz cell with a step size of 1 nm, a bandwidth of 1 nm and an averaging time of 4 s. The protein concentration was 0.1 mg/ml (≈3.6 μM) in 5 mM phosphate buffer, pH 7.5 in the absence and in the presence of 0.6 mM L-arginine, and in the presence of different concentrations of guanidine hydrochloride (GdmCl). For all spectra, an average of five scans was obtained.

CD spectra of the buffers were recorded and subtracted from the protein spectra. Heating from 20 °C to 95 °C was performed with a scan rate of 30 °C/h and the values of ellipticity at 222 nm were recorded every 0.5 °C. Concentration of GdmCl was determined by refractive index with a Abbe refractometer [22].

2.5. Intrinsic phosphorescence and fluorescence of TmArgBP

Typically, before all the experiments, TmArgBP samples were dialyzed overnight against 5 mM phosphate buffer, pH 7.5 with six buffer exchanges and the final protein concentration was of around 10 μM. For low-temperature studies, the samples contained 60% (v/v) glycerol. Experiments were performed in the absence and in the presence of L-arginine and in the absence and in the presence of 4 M and 8 M of urea. Protein samples were placed into a 5×5 mm^2 quartz cuvette, deoxygenated by cycles of vacuum followed by inlet of a stream of pure N_2, as previously described [23]. Fluorescence and phosphorescence spectra and decays were all measured with pulsed excitation (λ_{ex} = 292 nm) on a homemade apparatus [23]. Pulsed excitation was provided by a frequency-doubled Nd/Yag-pumped dye laser (Quanta System, Milan, Italy) with pulse duration of 5 ns and a typical energy per pulse of 0.5–1 mJ. Emission spectra were collected at 90° from the excitation and dispersed by 0.3 m focal length triplet grating imaging spectrograph (SpectraPro-2300i, Acton Research Corporation, Acton, MA) with a band-pass of 0.2 nm for low T spectra and of 1.0 nm for room T spectra. The emission was monitored by a back-illuminated 1340 × 400 pixels CCD camera (Princeton Instruments Spec-10:400B (XTE), Roper Scientific Inc., Trenton, NJ) cooled to −60 °C. In low temperature glasses, the phosphorescence spectrum was recorded after a 2 s delay from the exciting pulse. Background of free Trp spectra was obtained by opening the mechanical shutter controlling the emission to the spectrograph after a delay of 2 s. In fluid solutions, spectra were recorded by integrating multiple excitation pulses at a repetition frequency up to 10 Hz. To block overlapping prompt fluorescence and short-lived background from the detector, laser excitation was synchronized to a fast mechanical chopper opening the emission slit 50 μs after the laser pulse. In general, less than 20 pulses were sufficient to obtain satisfactory *S*/*N* ratios.

Phosphorescence decays were monitored by collecting the emission at 90° from vertical excitation through a filter combination with a transmission window of 405–445 nm (WG405, Lot-Oriel, Milano Italy, plus interference filter DT-Blau, Balzer, Milano, Italy). The photomultiplier (EMI 9235QA, Middlesex, UK) was protected against fatigue from the strong excitation/fluorescence pulse by the mechanical chopper synchronized to the laser trigger, which closed the emission slit during the excitation pulse. The time resolution of this apparatus depends on the chopper speed and, for the experiments reported here, was maintained constant to 50 μs, the same as for spectral acquisitions. The photocurrent was amplified by a current-to-voltage converter (SR570, Stanford Research Systems, Stanford, CA) and digitized by a 16 bits high speed (1.25 MHz) multifunction data acquisition board (NI 6250 PCI, National Instrument Italy, Milano, Italy) supported by LabVIEW software capable of averaging multiple sweeps. Typically, less than 20 sweeps were sufficient for a good signal-to-noise ratio even for the shortest decays. Prompt fluorescence was simultaneously collected through a 310–375 band-pass filter combination (WG305 nm plus Schott UG11) and detected by a UV-enhanced photodiode (OSD100-7, Centronics, Newbury Park, CA). An analogue circuit was used to integrate the photocurrent and its output was digitized and averaged by a multifunctional board (PCI-20428, Intelligent Instrumentation, Tucson, Texas) utilizing LabVIEW software. The prompt fluorescence intensity was used to account for possible variations in the laser output between measurements as well as to obtain fluorescence normalized phosphorescence intensities. All phosphorescence decays were analyzed in terms of a sum of exponential components by a nonlinear least-squares fitting algorithm (DAS6, fluorescence decay analysis software, Horiba Jobin Yvon, Milano, Italy). Each spectral and lifetime determination was repeated at least three times. Acrylamide quenching experiments were also performed and carried out as described before [24].

3. Results and discussion

3.1. Differential scanning calorimetry

Fig. 1A reports the thermal denaturation trace of the TmArgBP and some tentative fitting approaches. The traces show an asymmetric endothermic peak with a maximum at high temperature (about 115 °C), in line with the expectation for such hyperthermophilic proteins. Because of the asymmetry, the simplest thermodynamic interpretation, namely, one step equilibrium denaturation had to be ruled out. A tentative complex interpretation, i.e. the insertion of an irreversible step or the possibility of a multi-domain unfolding, was also excluded since it did not give satisfactory fits in any case. A satisfactory result was instead obtained with a very simple equilibrium model (see experimental procedures) that implies one-step dissociation of a homo-dimeric protein coupled with a one-step denaturation of the monomers.

$$N_2 \leftrightarrow 2U$$

This model allows us to single out the van't Hoff denaturation enthalpy of each monomer, ΔH^{vH}, which is the relevant thermodynamic parameter used to characterize the enthalpic contribution to the protein stability. This satisfactory fitting is in line with previous findings on the dimeric status of this protein even under strong denaturing conditions [12]. On the other hand, although the presence of structural domains is detectable and reported in the literature, our findings suggest that only one energetic domain is present in each monomer and that the presence of L-arginine increases the overall stability of the protein.

Fig. 1B shows the thermal denaturation traces (grey lines) and the fitting curves (black lines) drawn according to the dimer dissociation model for wild type protein with and without the presence of L-arginine. The overall denaturation mechanism in the presence of L-arginine remains the same as in the wild type and the dissociation model fits well in both cases. The maximum of the DSC signal, T_{max}, and the calculated values of ΔH^{vH} (monomer) are reported in Table 1.

3.2. Circular dichroism

In Fig. 2, far-UV CD spectra of TmArgBP at 20 °C in the absence and in the presence of L-arginine are reported. As it was previously demonstrated [11], the binding of L-arginine to TmArgBP induces small changes in the secondary structure content of the protein. The recorded CD data are in good agreement with this, being only detected a small effect on spectrum profile of the protein upon ligand binding.

In order to evaluate the content of secondary structure of the protein, we analyzed the far-UV CD spectra using the k2d algorithm [25]. The analysis revealed that the protein structure content consisted approximately of 36% α-helices and 14% β-sheets for TmArgBP, which is consistent with the three-dimensional model of the protein [11]. The binding of L-arginine to TmArgBP results in a small variation of the α and β protein structures content that is estimated to become 32% and 17%, respectively.

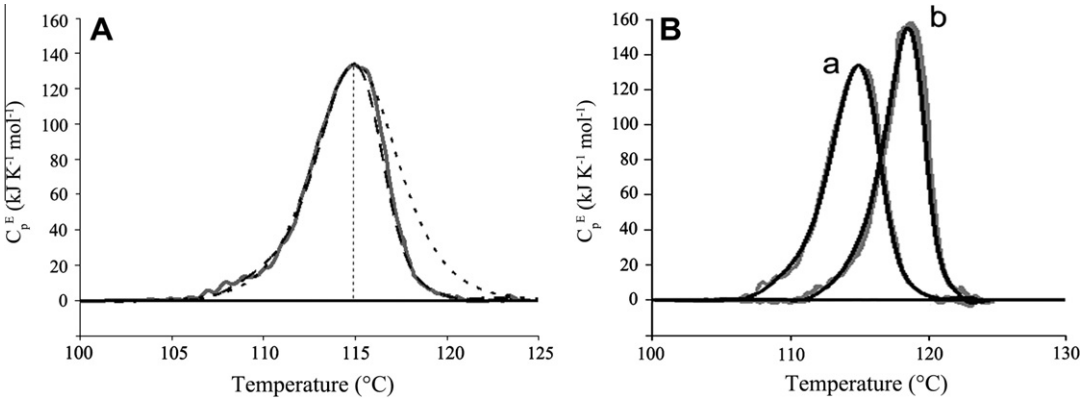

Fig. 1. (A) Experimental (continuous line) and theoretical DSC thermal denaturation curves of TmArgBP. The theoretical curves were calculated according to the single step denaturation (dotted line) and the dissociation models (dashed line). (B) Experimental (grey) and theoretical (black) DSC thermal denaturation curves. In the figure the wild type protein in the absence and in the presence of L-arginine (a and b, respectively) are reported. The theoretical curves were calculated by the dissociation model. Conditions: 5 mM phosphate buffer, pH 7; protein concentration 1.0 mg/ml; L-arginine/protein ratio (r); r = 477 for the TmArgBP + L-arginine system. 0.5 °C/min scan rate.

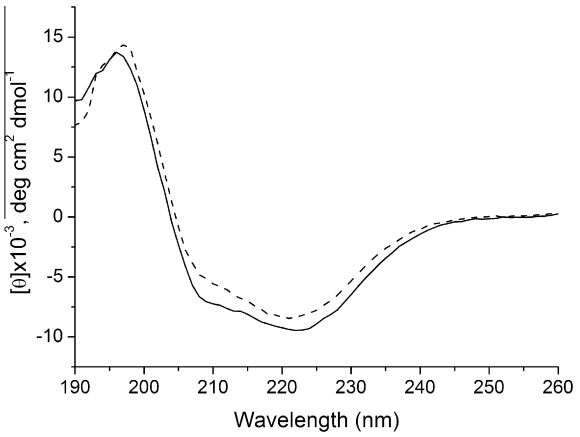

Fig. 2. Far-UV CD spectra of TmArgBP in the absence and in the presence of L-arginine (solid and dashed line, respectively) in 5 mM phosphate buffer, pH 7.5 at 20 °C. The protein solutions were at 0.1 mg/ml and L-arginine concentration was 0.6 mM. Spectra were recorded in the 260–190 nm spectral range in a 1 mm path length cell.

The stability of TmArgBP structure in the absence and in the presence of increasing amounts of GdmCl was investigated by CD experiments (Fig. 3). At 20 °C high concentrations of GdmCl are needed to induce relevant changes in TmArgBP secondary structure content. A complete denaturation of the protein can be detected at the highest GdmCl concentration reached in our experiments (7.8 M). In the presence of 2.6 M GdmCl and at 95 °C the CD spectrum of TmArgBP shows a totally random structure profile (Fig. 3). The binding of L-arginine to TmArgBP leads to an increase of the stability of the protein as revealed by the absence of a complete protein denaturation pattern at 20 °C, even in the presence of 7.8 M GdmCl. The complete thermal unfolding of the protein was recorded at 95 °C in the presence of 3.9 M GdmCl.

Thermal unfolding curves of TmArgBP at different GdmCl concentrations were obtained by monitoring the ellipticity at 222 nm as a function of temperature (Fig. 4). In agreement with the data reported in Fig. 3, at 95 °C it is observed that the complete protein unfolding process is reached in the presence of 2.6 M GdmCl. The binding of L-arginine increases the protein stability.

In all cases, a cooperative thermal unfolding process is observed with a transition temperature that decreases with increasing GdmCl concentrations up to 7.8 M. At specific concentrations of GdmCl, increasing the temperature from 20 °C to 95 °C results in unfolding of the protein structure through an apparent two-state mechanism both in the absence and in the presence of L-arginine. The different degrees of protein thermo-stability were also compared by the estimation of the melting temperature (T_m) in the presence of 3.9 M GdmCl. This concentration value of GdmCl allows for a visualization of the denaturation curve from the folded to the unfolded state of the protein samples. The values of T_m at this concentration value of GdmCl are 73.2 and 79.2 °C for ArgBP and ArgBP with L-arginine, respectively.

3.3. Emission characteristics of Trp^{226}

From low temperature emission spectra analysis in glycerol/buffer glasses, it appears that the phosphorescence spectrum is well structured (Fig. 5A), which is indicative of homogeneity in the Trp environment. Although the $\lambda_{0,0}$ peak is at 407.2 nm, which is the same wavelength as free Trp in this solvent, the bandwidth (the width at half height) is relatively narrow (4.42 nm c.f. to 9.5 nm for solvent exposed Trp) implying that the indole ring is largely buried within the protein fold [26]. The spectrum of Trp^{226} is blue shifted for an internal residue, which are often located near moderately polar sites. These values are also possible if the ground state energy, $E(S_0)$, is lowered by attractive interactions with nearby charges.

As shown in Fig. 5A, the phosphorescence spectrum remains relatively well resolved in 5 mM phosphate buffer, pH 7.5 at 20 °C. Moreover, it undergoes to a limited red-shift upon thermal relaxation of the surrounding structure ($\lambda_{0,0}$ shifts from 407.2 to 409.9 nm c.f. to 414–416 nm for solvent exposed or flexible sites). This is consistent with a relatively ordered and rigid site, again confirming little if any exposure of the indole ring to the solvent. The fluorescence spectrum of the protein is peaked at 338 nm having relaxed from F_{max} = 226 nm in rigid glasses (Fig. 5B). The red-shift on thermal relaxation is significant but much less than expected for solvent exposed or flexible sites. Since a very small spectral shift would be expected upon structural relaxation for non-polar sites, we infer that the Trp environment of the protein is polar and rather rigid.

The phosphorescence decays in buffer are homogeneous, consistent with uniformity in the Trp environment/dynamical structure in the millisecond time scale. The lifetime is 8.4 ms at 0 °C and 3.4 ms at 20 °C. This τ is long with respect to a Trp exposed to the solvent but it is still short for an internal protein rigid site. The lifetime is indicative of a superficially buried Trp residue where the indole ring is not in direct contact with the aqueous

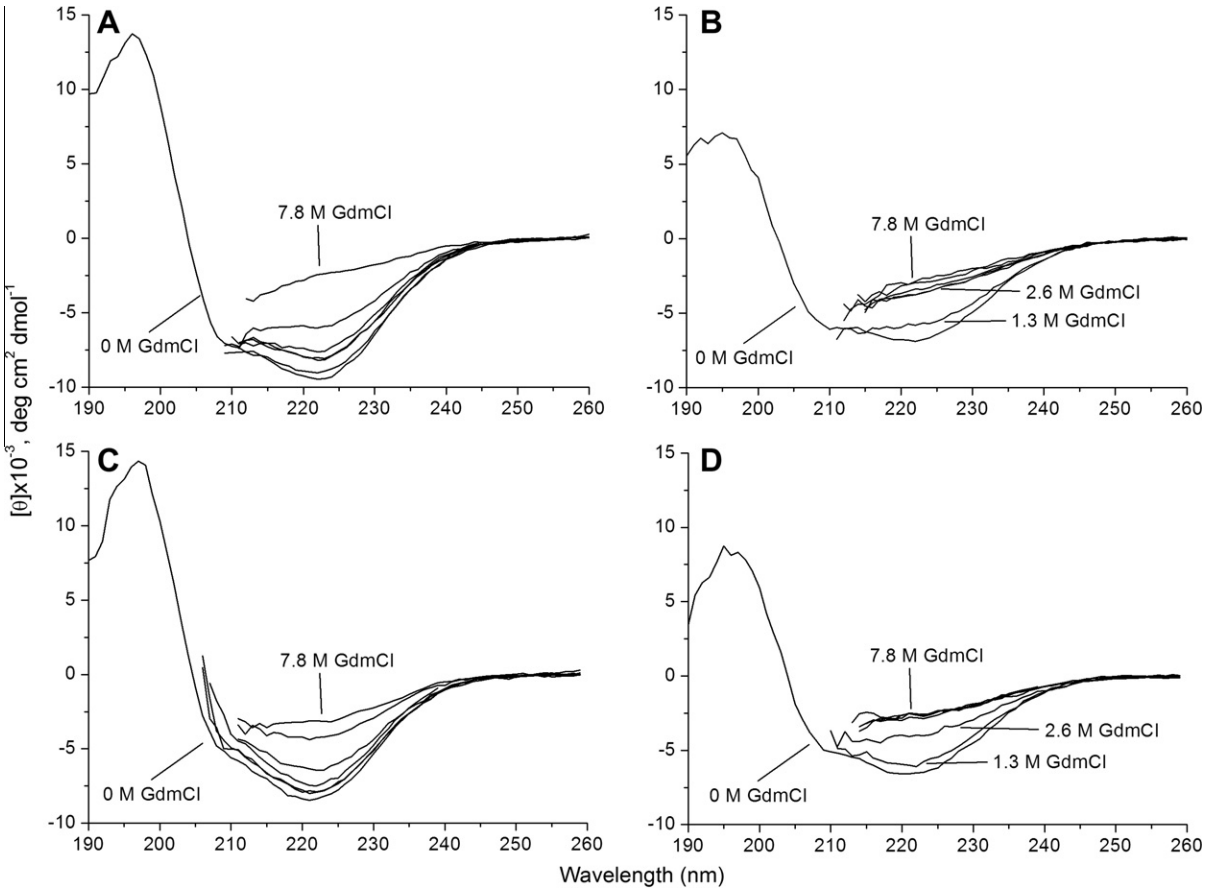

Fig. 3. Changes of far-UV CD spectra of TmArgBP in the absence and in the presence of L-arginine induced by increasing amount of GdmCl at 20 °C (panel A and C, respectively) and 95 °C (panel B and D, respectively). The protein solutions were at 0.1 mg/ml and L-arginine concentration was 0.6 mM while the GdmCl concentration was increased from 0 to 7.8 M with 1.3 M concentration increments. Spectra in the presence of GdmCl were recorded from 260 to 210 nm, cell path length was 1 mm.

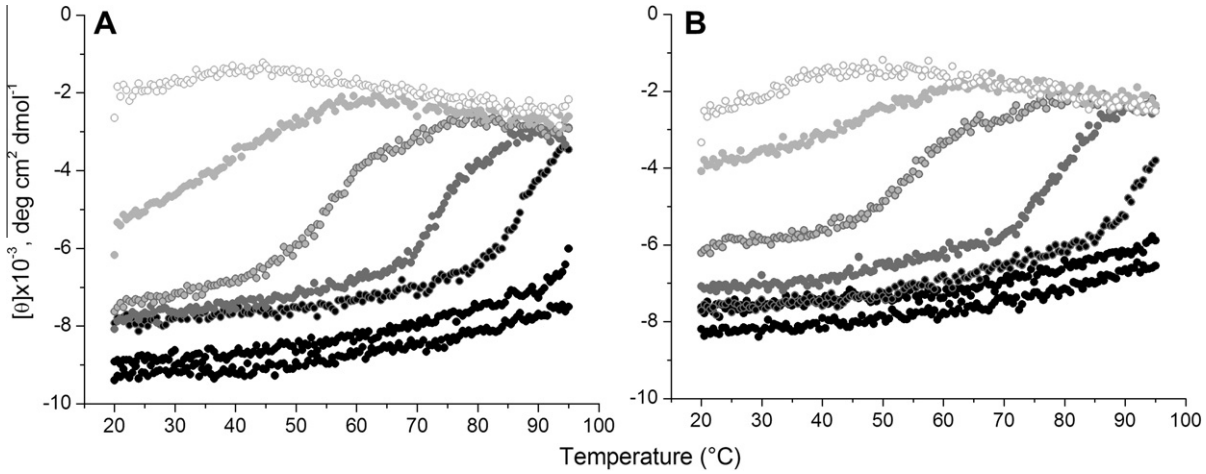

Fig. 4. Temperature dependence of ellipticity at 222 nm at pH 7.5 of TmArgBP (A), and TmArgBP with L-arginine (B), in the presence of different concentrations of GdmCl: grey scale of symbols is proportional to GdmCl concentration, from 0 M (black circles) to 7.8 M (white circles) with 1.3 M increments.

phase, but it is very near to it. This indicated that it can be effectively quenched by any quencher impurity in the solvent and/or by the His tail of the protein. It may be possible that the true intrinsic lifetime, which reflects the site flexibility [27], may be longer than the measured value.

We measured the effect of pH in the range between 5 and 10 on TmArgBP τ. At acid pH the TmArgBP τ decreases by 2–3-fold but there is little further variation above pH 7.5. Since His residues are stronger quenchers in the protonated state, it is possible that the τ reduction at acid pH is due to quenching by the protein His tag. However, the independence of τ on the protein concentration (reduced from 10 to 3 μM) suggests that the process is not intermolecular.

Quenching analysis of the protein Trp^{226} phosphorescence by acrylamide was performed. The gradient of the Stern–Volmer lifetime plot yields quenching rate constants of (1.02 and

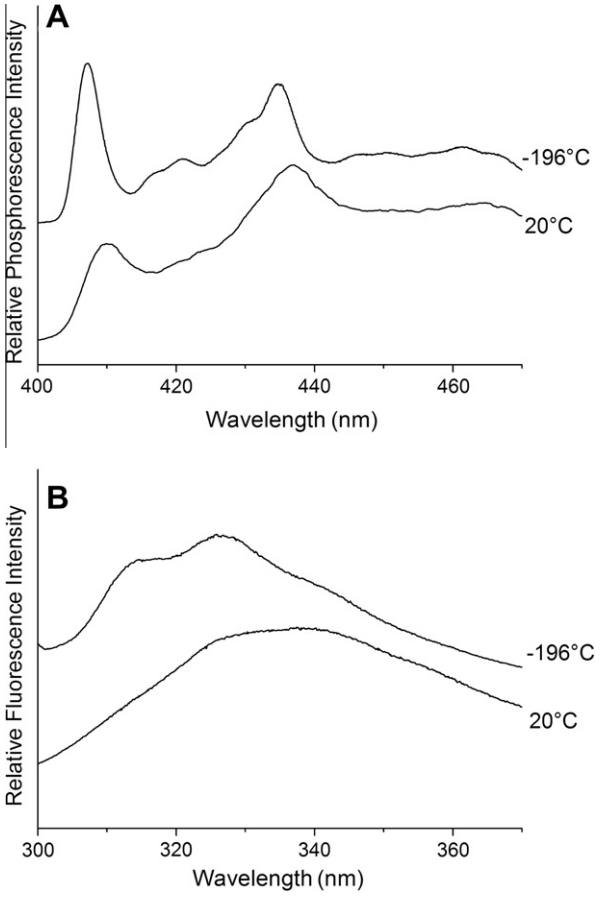

Fig. 5. Trp phosphorescence (panel A) and fluorescence (panel B) spectra of TmArgBP in a glycerol/buffer glass at −196 °C and in buffer at 20 °C. The protein concentration was 10 μM. Spectral intensities are offset for clarity.

1.77) × 10^8 $M^{-1}s^{-1}$, at 0 and 20 °C, respectively. This value is large indicating that Trp^{226} is readily accessible to acrylamide quenching (c.f. kq = 1.5 × 10^9 for NATA and 10^4–10^5 for the Trp of RNaseT1 and parvalbumin, which are buried 2–3 Å from the aqueous interface [28]). Hence, if Trp^{226} is not directly exposed to the solvent then it must be very near to it (<0.5 Å) in order for acrylamide quenching from the solvent be so efficient. In order to estimate the effect of the protein subunit dissociation in the Trp microenvironment, τ value in 4.0 M and 8.0 M urea was measured. It was found that there is a modest reduction of the protein lifetime. However, as the lifetime reduction is small and is observed also in 4 M urea, which is insufficient to dissociate the oligomer, it is important to consider that this lifetime shorting may be due to the presence of impurities present in urea solution.

Since no changes were observed in the protein fluorescence spectrum we can conclude that the region of Trp^{226} is not involved in the association of the subunits and also that monomer formation has no significant impact on the protein structure near the indolic residue.

None of the various spectroscopic features examined is detectably affected by L-arginine binding to the protein. This is a highly surprising result especially since the binding process involves a large structural rearrangement as the rotation-closing of the two domains. As evident in Fig. 6, no changes are present in phosphorescence (panel A) and fluorescence spectra (panel B) and in phosphorescence decay (panel C) in the absence and in the presence of L-arginine.

In our best knowledge, this is the first protein that does not report changes in phosphorescence emission upon ligand binding. This suggests that not only the binding site is far from Trp^{226} but

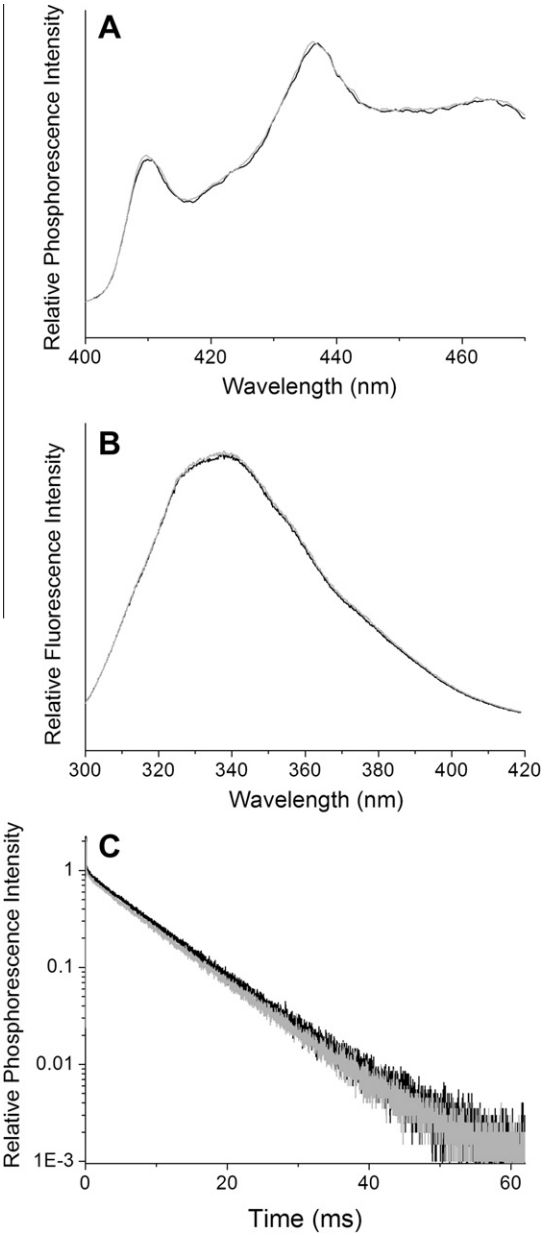

Fig. 6. Effect of L-arginine on Trp phosphorescence (panel A), fluorescence (panel B) and phosphorescence decay (panel C) at 20 °C. Black and grey curves represent TmArgBP in the absence and in the presence of L-arginine, respectively.

also that its local structure/dynamics is totally disconnected from the binding site region.

3.4. Analysis of Trp^{226} microenvironment by using the TmArgBP predicted structure

From the analysis of the interactions involving the Trp^{226} microenvironment and based on the predicted structure of TmArgBP [11], it is possible to notice the presence of stabilizing interactions between the carboxyl group of Asp^{39} facing the positive end of the Trp^{226} indole dipole (N1) (atomic length = 3.0 Å) and between the positive charge of Lys^{225} facing the negative end of the Trp^{226} dipole (C4–C5) (atomic length = 4.2 Å). In the closed form, it seems that the microenvironment of Trp^{226} does not undergo evident changes (Fig. 7) and the interaction distances remain roughly unvaried which is consistent with our hypothesis that the structural changes due to the adoption of the closed conformation does

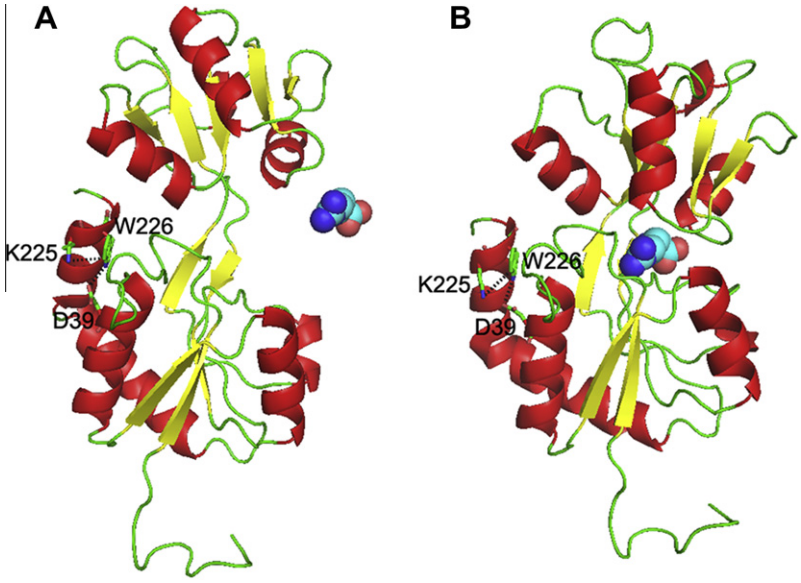

Fig. 7. 3D cartoon models of open (A), and closed (B) TmArgBP forms. Trp^{226} and amino acids which interact with Trp^{226} are displayed in sticks and labeled. L-arginine is displayed in spheres and the black dashed lines represent the amino acid distances. The PDB models were previously generated by Scire et al. [11] and displayed by PyMOL (version 1.1 eval) [32].

not involve Trp^{226} and its microenvironment. However, the different conformations of the open and closed forms could be used to detect the presence of L-arginine. Using the protein three-dimensional model, strategic amino acid residues could be mutated in order to make TmArgBP optically sensitive to the presence of L-arginine detectable by the presence of a new fluorescent intrinsic residue or by the introduction of an appropriate fluorescent probe that allows for the transduction of the ligand-binding event into a quantifiable optical signal variation.

In conclusion, TmArgBP was previously cloned, purified and partially characterized [11,12,29]. Some of its peculiar features investigated in this work such as the high specificity for the binding L-arginine and the extreme stability to high temperature could make this protein a perfect scaffold for the design of a new optical fluorescent biosensor for the detection of L-arginine [16,30].

In fact, a novel method for a fast real-time and continuous detection an of L-arginine in plasma, serum and urine would be of high interest to prevent the consequences of hyper-argininemia on health, especially in neonatal age [31].

4. Abbreviations

DSC	differential scanning calorimetry
TmArgBP	arginine-binding protein from *Thermotoga maritima*
GdmCl	guanidine hydrochloride
CD	circular dichroism

Acknowledgments

This work was in the frame of the CNR Commessa AGP05. The authors wish to thank Dr. Giovanni Strambini and Dr. Margherita Gonnelli for the phosphorescence measurements.

Appendix A. Supplementary material

Supplementary data associated with this article can be found, in the online version, at http://dx.doi.org/10.1016/j.jphotobiol.2012.11.004.

References

[1] G.F. Ames, Bacterial periplasmic transport systems: structure, mechanism, and evolution, Annu. Rev. Biochem. 55 (1986) 397–425.
[2] A.S. Ethayathulla, Y. Bessho, A. Shinkai, B. Padmanabhan, T.P. Singh, P. Kaur, S. Yokoyama, Purification, crystallization and preliminary X-ray diffraction analysis of the putative ABC transporter ATP-binding protein from *Thermotoga maritima*, Acta Crystallogr. Sect. F Struct. Biol. Cryst. Commun. 64 (2008) 498–500.
[3] C.F. Higgins, ABC transporters: from microorganisms to man, Annu. Rev. Cell Biol. 8 (1992) 67–113.
[4] R. Tam, M.H. Saier Jr., Structural, functional, and evolutionary relationships among extracellular solute-binding receptors of bacteria, Microbiol. Rev. 57 (1993) 320–346.
[5] A.L. Davidson, E. Dassa, C. Orelle, J. Chen, Structure, function, and evolution of bacterial ATP-binding cassette systems, Microbiol. Mol. Biol. Rev. 72 (2008) 317–364 (table of contents).
[6] M.J. Cuneo, A. Changela, A.E. Miklos, L.S. Beese, J.K. Krueger, H.W. Hellinga, Structural analysis of a periplasmic binding protein in the tripartite ATP-independent transporter family reveals a tetrameric assembly that may have a role in ligand transport, J. Biol. Chem. 283 (2008) 32812–32820.
[7] J.C. Pickup, F. Hussain, N.D. Evans, O.J. Rolinski, D.J. Birch, Fluorescence-based glucose sensors, Biosens. Bioelectron. 20 (2005) 2555–2565.
[8] D.E. Benson, D.W. Conrad, R.M. de Lorimier, S.A. Trammell, H.W. Hellinga, Design of bioelectronic interfaces by exploiting hinge-bending motions in proteins, Science 293 (2001) 1641–1644.
[9] U. Wissenbach, S. Six, J. Bongaerts, D. Ternes, S. Steinwachs, G. Unden, A third periplasmic transport system for L-arginine in *Escherichia coli*: molecular characterization of the artPIQMJ genes, arginine binding and transport, Mol. Microbiol. 17 (1995) 675–686.
[10] R. Huber, T.A. Langworthy, H. König, M. Thomm, C.R. Woese, U.B. Sleytr, K.O. Stetter, *Thermotoga maritima* sp. nov. represents a new genus of unique extremely thermophilic eubacteria growing up to 90 °C, Arch. Microbiol. 144 (1986) 324–333.
[11] A. Scire, A. Marabotti, M. Staiano, L. Iozzino, M.S. Luchansky, B.S. Der, J.D. Dattelbaum, F. Tanfani, S. D'Auria, Amino acid transport in thermophiles: characterization of an arginine-binding protein in *Thermotoga maritima*. 2. Molecular organization and structural stability, Mol. Biosyst. 6 (2010) 687–698.
[12] M.S. Luchansky, B.S. Der, S. D'Auria, G. Pocsfalvi, L. Iozzino, D. Marasco, J.D. Dattelbaum, Amino acid transport in thermophiles: characterization of an arginine-binding protein in *Thermotoga maritima*, Mol. Biosyst. 6 (2010) 142–151.
[13] S.W. Brusilov, A.L. Horwich, Urea cycle enzymes, in: C.R. Scriver, A.L. Beaudet, W.S. Sly, D. Valle (Eds.), The Metabolic Basis of Inherited Disease, McGraw-Hill, New York, 1989, pp. 629–663.
[14] H.W. Hellinga, J.S. Marvin, Protein engineering and the development of generic biosensors, Trends Biotechnol. 16 (1998) 183–189.
[15] O.V. Stepanenko, A.V. Fonin, K.S. Morozova, V.V. Verkhusha, I.M. Kuznetsova, K.K. Turoverov, M. Staiano, S. D'Auria, New insight in protein-ligand interactions. 2. Stability and properties of two mutant forms of the D-galactose/D-glucose-binding protein from *E. coli*, J. Phys. Chem. B 115 (2011) 9022–9032.

[16] Y. Tian, M.J. Cuneo, A. Changela, B. Hocker, L.S. Beese, H.W. Hellinga, Structure-based design of robust glucose biosensors using a *Thermotoga maritima* periplasmic glucose-binding protein, Protein Sci. 16 (2007) 2240–2250.
[17] V. Scognamiglio, M. Staiano, M. Rossi, S. D'Auria, Protein-based biosensors for diabetic patients, J. Fluoresc. 14 (2004) 491–498.
[18] G. Barone, P. Del Vecchio, D. Fessas, C. Giancola, G. Graziano, Theseus: a new software package for the handling and analysis of thermal denaturation data of biological macromolecules, J. Therm. Anal. 38 (1992) 2779–2790.
[19] S. D'Auria, R. Barone, M. Rossi, R. Nucci, G. Barone, D. Fessas, E. Bertoli, F. Tanfani, Effects of temperature and SDS on the structure of beta-glycosidase from the thermophilic archaeon *Sulfolobus solfataricus*, Biochem. J. 323 (Pt 3) (1997) 833–840.
[20] D. Fessas, S. Iametti, A. Schiraldi, F. Bonomi, Thermal unfolding of monomeric and dimeric beta-lactoglobulins, Eur. J. Biochem. 268 (2001) 5439–5448.
[21] W.H. Press, B.P. Flannery, S.A. Teukolsky, W.T. Vetterling, in: C.U. Press (Ed.), Numerical recipes: The art of scientific computing, Cambridge, UK, 1989, pp. 521–538.
[22] Y. Nozaki, The preparation of guanidine hydrochloride, Methods Enzymol. 26 PtC (1972) 43–50.
[23] G.B. Strambini, B.A. Kerwin, B.D. Mason, M. Gonnelli, The triplet-state lifetime of indole derivatives in aqueous solution, Photochem. Photobiol. 80 (2004) 462–470.
[24] P. Cioni, G.B. Strambini, Acrylamide quenching of protein phosphorescence as a monitor of structural fluctuations in the globular fold, J. Am. Chem. Soc. 120 (1998) 11749–11757.
[25] M.A. Andrade, P. Chacon, J.J. Merelo, F. Moran, Evaluation of secondary structure of proteins from UV circular dichroism spectra using an unsupervised learning neural network, Protein Eng. 6 (1993) 383–390.
[26] M.V. Hershberger, A.H. Maki, W.C. Galley, Phosphorescence and optically detected magnetic resonance studies of a class of anomalous tryptophan residues in globular proteins, Biochemistry 19 (1980) 2204–2209.
[27] M. Gonnelli, G.B. Strambini, Phosphorescence lifetime of tryptophan in proteins, Biochemistry 34 (1995) 13847–13857.
[28] G.B. Strambini, M. Gonnelli, Protein phosphorescence quenching: distinction between quencher penetration and external quenching mechanisms, J. Phys. Chem. B 114 (2010) 9691–9697.
[29] A. Ruggiero, J.D. Dattelbaum, A. Pennacchio, L. Iozzino, M. Staiano, M.S. Luchansky, B.S. Der, R. Berisio, S. D'Auria, L. Vitagliano, Crystallization and preliminary X-ray crystallographic analysis of ligand-free and arginine-bound forms of *Thermotoga maritima* arginine-binding protein, Acta Crystallogr. Sect. F Struct. Biol. Cryst. Commun. 67 (2011) 1462–1465.
[30] M. Strianese, M. Staiano, G. Ruggiero, T. Labella, C. Pellecchia, S. D'Auria, Fluorescence-based biosensors, Methods Mol. Biol. 875 (2012) 193–216.
[31] S. Jain-Ghai, S.C. Nagamani, S. Blaser, K. Siriwardena, A. Feigenbaum, Arginase I deficiency: severe infantile presentation with hyperammonemia: more common than reported?, Mol Genet. Metab. 104 (2011) 107–111.
[32] W. DeLano, The PyMOL Molecular Graphics System, in, DeLano Scientific LLC., Palo Alto, California, USA, 2008, pp. <http://www.pymol.org>.